Study on b-Value Characteristics of Acoustic Emission of Cemented Waste Rock Backfills during Short-Term Creep Process

Li Changhong[1,2], Ma Qiantian[1,2], Mao Tianwei[3]

1 Key Laboratory of the Ministry of Education of China for High-efficient Mining and Safety of Metal Mines, University of Science and Technology Beijing , Beijing, 100083, China
2 School of Civil and Environmental Engineering, University of Science and Technology Beijing, Beijing, 100083, China
3 Mining Branch of Meishan Iron & Steel Co, Nanjing, Jiangsu, 210041, China

Corresponding author is Ma Qiantian

Abstract
Shear failure and tensor failure are two kinds of failure modes of cemented waste rock backfills. The studies on b-value characteristics of acoustic emission of blocky rock cemented fill with two kinds of failure modes during creep process were carried out by virtue of short-term creep test under step constant load. The results show that: The fluctuation of b-value is like upward serration as the two kinds of specimens are in steady creep stage before the specimen failure. As the Shear failure specimen in tertiary creep stage b-value of acoustic emission shows a circulation pattern that is "upward serrated fluctuation with decreased intensity"; whereas as the tensor failure specimen in tertiary creep stage b-value of acoustic emission shows a continuing upward serrated fluctuation with increased amplitude. Therefore, the cemented waste rock backfills failure can be forecasted by the variation characteristics of b-value to some extent.
Keywords: CEMENTED WASTE ROCK BACKFILLS, SHORT-TIME CREEP, ACOUSTIC EMISSION, B-VALUE

1. Instruction

Currently in many mines, to fully recover resources, the mining order of first pillars and filling and then rooms is adopted. Especially for rare and precious metal mines (such as gold mines and silver mines, etc.), implement stoping of top sill pillars and studs in the first stage in order to improve the ore recovery rate. Fill cemented filling formed by barren rocks and tailings into the artificial ore pillars. In the second stage, rooms are stoped. Therefore, in the room stoping process, cemented waste rock backfills will replace native pillars as the main support. With large areas of stoping in native ores, these ores' solid wastes are added with cementing materials, thus forming cemented backfills. These cemented backfills play a key role as the main support for safety stoping of mines and can effectively control ground pressure. In case of any instability or damage, it will cause the collapse and sink of the roof, rock movement of the upper and lower sides, or even induce the occurrence of deep stoping rock burst, which will become a serious threat to secure stoping. Hence, in recent years, the new engineering material of cemented solid waste mine backfills has attracted considerable attention [1]. It is hoped that it can provide an important basis for filling material selection, optimization and stability analy-

sis when making an investigation into the mechanical properties and damage mechanism of cemented solid waste backfills in a complex environment. Further, it aims to propose the filling body stability monitoring and prediction methods on this basis. For example, through a waste rock tailings backfill test, Guo Lijie measured the feature parameters of backfill mechanics and advocated that in comparison with tailings, waste rocks had outstanding advantages in improving intensity of the backfilling [2]. Liu Zhixiang analyzed the deformation and failure characteristics of the backfills with different mixture ratios by tail sand cemented mechanical tests with different mixture ratios and established backfill damage constitutive equations with four different mixture ratios [3]. Wang Xiaojun analyzed the relationship between the compressive strength and the acoustic velocity of cemented tailings backfills by experiments and established a mathematical model of the longitudinal wave velocity and uniaxial compressive strength of the backfills [4]. Deng Daiqiang and Gao Yongtao established a function between confining pressure and energy consumption of cemented tailings backfills with different mixture ratios on a trial basis [5]. Meanwhile, on the basis of existing research, acoustic emission can qualitatively or quantitatively describe the evolution behaviors of micro-crack of concrete and concrete-like material due to the external loading condition [6,7], and can predict its occurrence of disasters. This technology has been gradually introduced. Wang Xiaojun and Feng Xiao studied the energy characteristics and spatial distribution rules of acoustic emission in the tailings backfill rupture process by employing the numerical model [8]. Gong Cong explored the b-value features of acoustic emission of tailings backfill under uniaxial cyclic loading and unloading conditions [9]. For waste rock cemented backfills as quasi-brittle materials like concrete and rocks, its damage failure is closely associated with acoustic emission. However, there is rare research in this regard.

With reference to waste rock cemented backfills, the inoculation, initiation, evolution, expansion and fracture processes of micro-fracture emerge between waste rocks. In this case, different spatial combinations of waste rocks will have different destabilization ways. Meanwhile, in continuous mining operating conditions, artificial pillars won't last long under certain constant load. Hence, this paper carried out an experiment of creep acoustic emission of waste rock cemented backfills with different destabilization ways under the short-term graded loading conditions. It has found the deformation rules and acoustic emission data of two types of specimens under constant load at all levels, and then studied the relationship between deformation characteristics and features of acoustic emission parameter changes of waste rock cemented backfills. The research findings has reference value to further reveal and forecast the destabilization premonition of waste rock cemented backfills.

2. Design of Experiment and Acquisition of Data

2.1. Experimental System

The test system consists of two parts: RMT-150C rock mechanics test system developed by Institute of Rock and Soil Mechanics, Chinese Academy of Sciences, BZ2005C static strain gauges developed by the Institute of Electrical Automation in Beidaihe and SAEU2S digital sound transmission system developed by Beijing Shenhua Industrial Technology Co., Ltd. RMT-150C rock mechanics test system has a maximum load of 1000 kN, a piston stroke of 50 mm, and frame stiffness of 5×106 N·mm-1. BZ2005C static strain gauge has a sensitivity factor of 2.0, measuring range of ± 19999 με, the minimum sampling interval of 20 s and the maximum storage capacity of 99 strain data. SAEU2S acoustic emission system is a multichannel acoustic emission system that can real-time acquire acoustic emission signals.

2.2. Specimens Preparation

The waste rocks in this test were taken from phyllite rocks in Yinshan. When many mines make artificial pillars, they do not use graded gravel, but crushing waste rocks, resulting in non-uniform waste rock particle sizes, and even great particle size for individual waste rocks. Therefore, in the production of cemented waste rock backfills, this paper divided them into two groups by the size. Particle size in one group was 5-31.5mm, while in another group was 31.5-50mm, in which the latter group has less than 10% of the use amount of waste rocks. Tailings were from a copper mine in Jiangxi Wushan, and prepared cement mortar with 325 # silicate, with cement-sand ratio of 1: 4 and the mass concentration of 75%. The specimen is a cylinder, with a size of φ75×150 mm. The model was removed of form 7 days after pouring and conserved for 28 days. A total of 20 specimens were obtained.

First of all, a uniaxial compression test was conducted on these 20 specimens of waste rock cemented backfills. As shown in Figure. 1, according to the instability ways of the test specimen, cemented waste rock backfill specimen is divided into two types: in Figure. 1 (a), when the left and right waste rock bodies in the specimen were combined in a small angle (smaller than 58°), the specimen would have shearing instability between two parts of waste rock com-

bination, hereinafter referred to as Type I, with the average compressive strength of 3.44MPA. In Figure 1. (b), when the left and right waste rock bodies in the specimen were combined in a large angle (larger than 58°), the specimen would have tensor instability between two parts of waste rock combination, hereinafter referred to as Type II, with the average compressive strength of 3.32MPa. In Figure. 1, a waste rock combination in the two sides of the centre joints is formed by cement-cemented tailings backfill material. The centre joint is located in the centre part of the specimen and penetrates through cement-tailings backfill layer of most of the specimens. For Type I, the centre joint is the macroscopic shear plane when the specimen is instable; for Type II, when the specimen is instable, it opens along the centre joint.

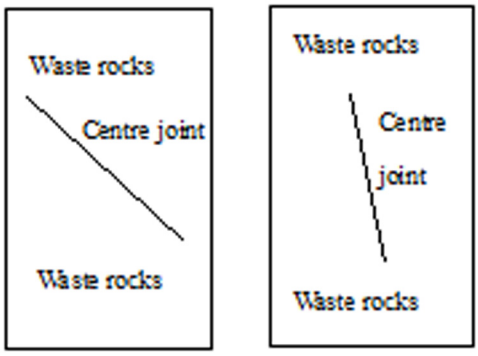

(a) Type I (b) Type II

Figure 1. Structure in Cemented Waste Rock Backfills

On the basis of the uniaxial test results, by controlling the angles of the centre joints, two types of cemented waste rock backfill specimens, 5 for each, participated in the short-term graded creep test. Wherein Type I specimens were numbered from 1~5, and Type II specimens were numbered from 6~10.

2.3. Design of Experiment

This test adopted the short-term graded creep test. 5-grade constant loading was carried out on the specimen according to the average uniaxial compressive strength measured, and the 1-grade to 5-grade stresses were 40%, 50%, 60 %, 70% and 80% of the average uniaxial compressive strength, and the loading rate was 0.1KN/S. Time for the graded load creep test to stabilize pressure is usually determined by the size of the specimen displacement amount: When the displacement amount of the specimen axial deformation in 2 d was less than 0.01 mm, it can move to the next loading. At the same time, long-term acoustic emission monitoring of the specimen can get effective data, but it would also bring some difficulties to store, extract and analyze the data. As a result, in the short-term graded creep test in this paper, the specimen can enter the next loading only when they have entered into the steady creep for one hour. The acoustic emission sensor is disposed in the middle axial part of the specimen, and attached to the specimen by using butter as the coupling agent. The sampling length of acoustic emission is set to 2048 Byte; the sampling frequency is 1000 KHz and the preamplifier gain is 40 dB. The model of acoustic emission sensor is SR150M; the operating frequency is 20 kHz ~ 400 KHz, and the center frequency is 150 KHz. Because the probe's radius for force loading in the test was smaller than the radius of the specimen, in order to guarantee equal force in the specimens, steel plates whose terminal area was larger than the specimen were added to both ends of the specimens.

2. Experimental Results of Deformation

For the entire creep stage, it can be qualitatively divided into three stages by the change feature that material deformation (strain) rate changes with time, namely the deceleration creep, steady creep and accelerating creep. This paper defines the corresponding time period when the axial strain rate stabilizes at a certain value as the steady creep stage, and the stage prior to it is the deceleration stage, while the stage after it is the accelerating creep stage.

In this paper, the strain of the specimen under compression state is defined as positive, while the strain of the specimen under tensile state is defined as negative. Formula (1) shows the calculation method of the specimen's volume strain:

$$\varepsilon_v = \varepsilon_z + 2\varepsilon_h \quad (1)$$

ε_v is volumetric strain, ε_z is axial strain and ε_h is transverse strain.

2.1. Experimental Results of Type I

In this type, specimen 3 was selected for related discussions. Figure. 2 shows the changes in axial strain, transverse strain, volumetric strain and the number of acoustic emission events of specimen 3 at all loads. As can be seen from the figure, the axial strain increment of specimen 3 at each level is mainly concentrated in the decelerating creep stage. However, as the constant load is increasing, the strain increment at this stage gets smaller and smaller. Finally, in the fifth constant load, specimen 3 shows accelerating creep and the strain increment increases dramatically. Nevertheless, under constant load at the first two levels, transverse strain of specimen 3 is not obvious. As the constant load is increasing, transverse strain of specimen 3 begins to appear, but its absolute value does not exceed the axial strain. In the acceleration creep stage, either strain increment or strain rate is far less than the axial strain.

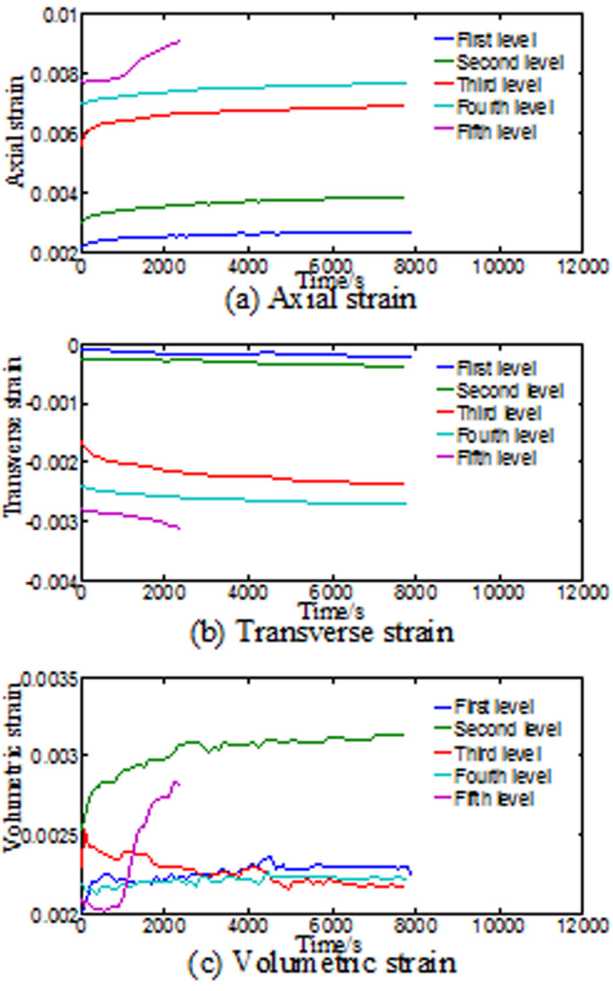

Figure 2. The creep curves of specimen 3

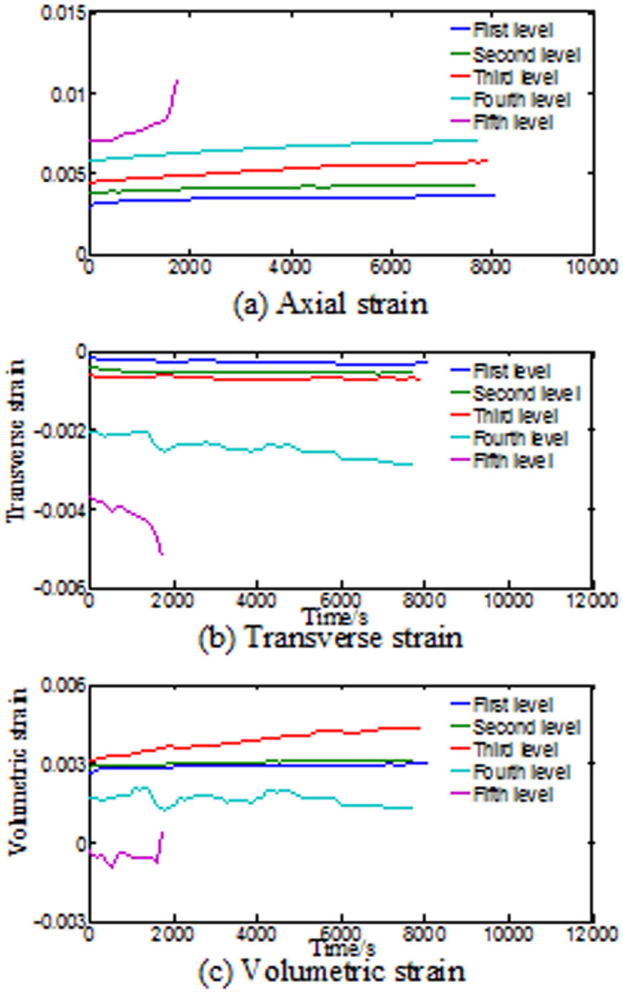

Figure 3. The creep curves of specimen 7

Under the first two constant loads of specimen 3, volumetric strain is on the rise and the value is positive, indicating that it is in volume deformation stage. Under the third constant load, volume strain of specimen 3 begins to gradually decrease and stabilizes at around 0.0025, indicating that it enters the volume constant stage. Finally, under the fourth and fifth constant loads, the volume strain increases again and the value is positive, indicating that it enters the volume deformation stage. Specimen 3 does not have dilatation throughout the testing process.

2.2. Experimental Results of Type II

In this type, specimen 7 was selected for related discussions. Figure. 3 shows the changes in axial strain, transverse strain, volumetric strain and the number of acoustic emission events of specimen 7 at all loads. As can be seen from the figure, the axial strain increment rule of specimen 7 at each level is resemble to that of specimen 3. Meanwhile, lateral strain of specimen 7 under the former three constant loads is not obvious. In the fourth constant load, significant changes could be observed in the transverse strain of specimen 7, but its absolute value still does not exceed the axial strain. Lastly, in the fifth constant load, accelerating creep occurs.

Under the former three constant loads, specimen 7 is in the volume deformation stage and it enters into the volume constant stage in the fourth constant load. Volume strain stabilizes at around 0.0013. However, in the fifth constant load, volumetric strain of specimen 7 turns negative in the decelerating creep and steady creep stages and it enters the dilatation phase.

3. Acoustic Emission b-Value Features

3.1. Principle of Acoustic Emission b-Value

As shown in Formula (2), the b-value is often used in the study of earthquakes to describe the relationship between magnitude and total number of earthquakes, which is Gutenberg-Richter relationship [10]:

$$\lg(N) = a - bM \tag{2}$$

where M is earthquake magnitude; N is total number of earthquakes in the scope of $M+\Delta M$; a is constant of seismic activity degree; b is the b-value in seismology, and it only applies to a certain range of magnitude range at the right side of the peak magnitude in the magnitude-frequency distribution. Be-

cause there is no concept of earthquake magnitude in acoustic emission, it can only use magnitude to replace amplitude to calculate the b-value, and evaluate the extension situation of cracks in the specimen through variation features of the b-value. In this paper, the least squares method is employed to obtain the b-value, where the amount of data sampling window is 10,000, a sliding window is 2000, and ΔM is 0.001dB.

Studies have shown that variation features of acoustic emission b-value may reflect evolution features of microcracks within the material [11-13]. If the acoustic emission b-value tends to be stable within a certain range, it indicates that the microcracks in the material expand stably, and if a sudden jump occurs drammatically in the b-value, it represents the microcracks within the material is intensely expanding; the gradual increase in b-value represents that the interior materials are mainly small-scale microfracture damage; on the contrary, it represents the microfracture in the internal materials is mainly large-scale destruction [14].

3.2. Acoustic Emission b-Value Features of Type I Specimen

Figure. 4 shows the acoustic emission b-value-axial strain curve of specimen 3 in the entire creep stage. It can be seen that in the constant load that does not cause specimen instability, there is a close relationship between acoustic emission b-value and volume strain of specimen 3. When the specimen is in the volume deformation stage, acoustic emission b-value shows a decreasing trend with the increase in the strain in the decelerating creep stage, indicating that the microcracks inside the specimen in the decelerating creep phase is mainly large-scale destruction. Also, it can be seen from Figure 4 and Table 1 that in decreasing and steady creep stage of the volume deformation stage as well as the entire volume constant stage, the overall acoustic emission b-value no longer significantly reduces, but fluctuates up and down. Besides, the variance is not large and both the mean and variance of the acoustic emission b-value are increasing as the dead load decreases, indicating that microcracks in the specimen are in a steady expansion stage in two stages, and extend more stably with the increase of dead load.

3.3. Acoustic Emission b-Value Features of Type II Specimen

Figure. 5 shows the acoustic emission b-value-axial strain curve of specimen 7 in the entire creep stage. It can be seen that the specimen in the decelerating and steady creep phases of the volume deformation stage, the specimen's acoustic volume b-value

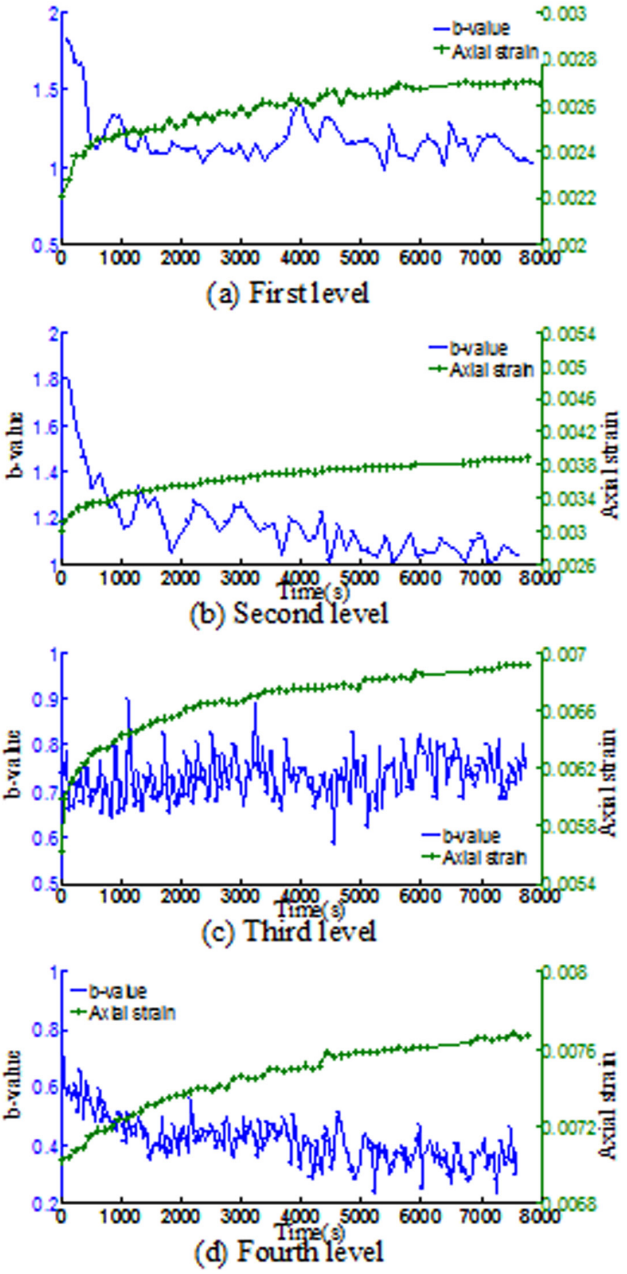

Figure 4. The b-value features of specimen 3

Table 1. The average value and variance of b-value in steady creep stage

Number	Steady creep	First level	Second level	Third level	Fourth level
3	Average value of b-value	1.1412	1.1125	0.7892	0.3873
	Variance of b-value	0.0074	0.0055	0.0037	0.0021
7	Average value of b-value	1.2416	1.0196	0.4265	0.3851
	Variance of b-value	0.0030	0.0058	0.0070	0.0048

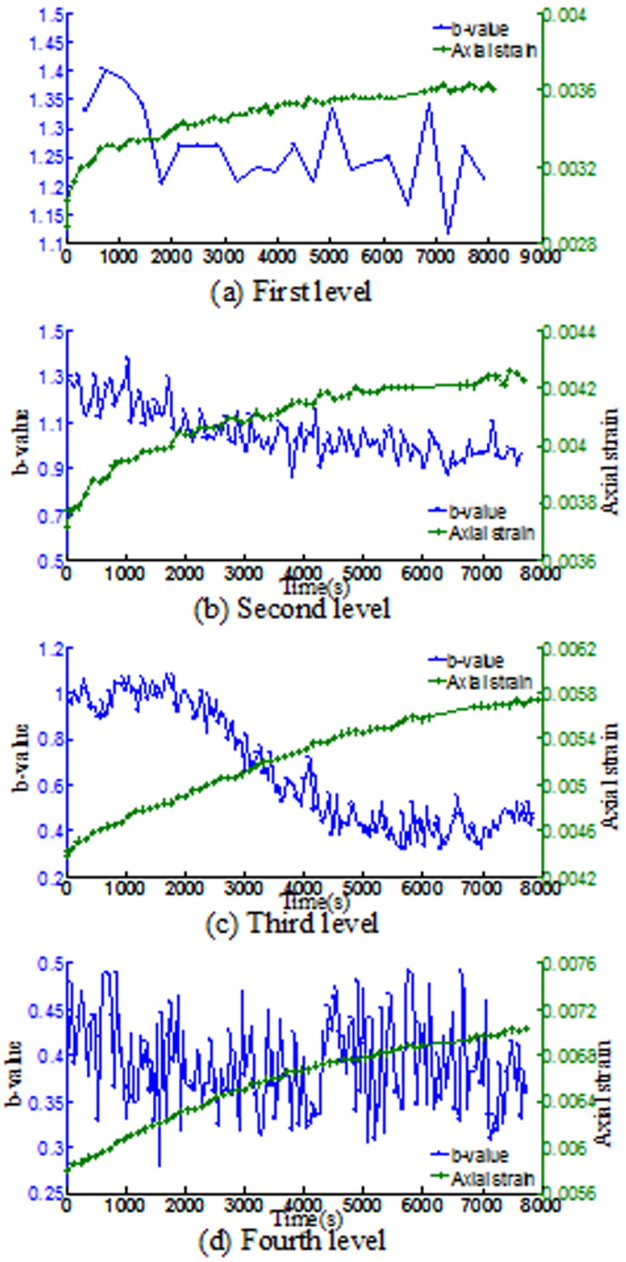

Fig 5. The b-value features of specimen 7

variation is the same as specimen 3. However, it can be seen from Figure. 5 and Table. 1 that in the steady creep stage of the volume deformation stage, although the overall acoustic emission b-value is stable, there is an increasingly enlarged variance, indicating that microcracks in the specimen in the steady creep stage of the volume deformation stage expand more dramatically with an increase in the dead load.

3.4. Acoustic Emission b-value Features before Specimens Instability

In order to achieve the purpose of predicting the instability of cemented waste rock backfills by acoustic emission b-value, it is necessary to get the acoustic emission b-value variation features before instability of cemented backfills. Among them, in the accelerating creep and pior steady creep stages, the acoustic emission b-value variation features are particularly important. Figure. 6 shows the creep acoustic emission b-value variation rules under the fifth grade of constant load of specimen 3 and specimen 7. The following characteristics can be found: acoustic emission b-values of two types of specimens in the steady creep stage gradually change to jagged upward fluctuations. In the fluctuations, acoustic emission b-values of Type I shows a decreasing trend while acoustic emission b-values of Type II shows an increasing trend. The acoustic emission b-value of Type I specimen in the accelerating creep stage shows a circulation pattern "jagged upward fluctuation - dramatic decrease"; The acoustic emission b-value of Type II specimen is maintained at contatnly up jagged fluctuations and in the fluctuations, it tends to increase, and enlarges the scale.

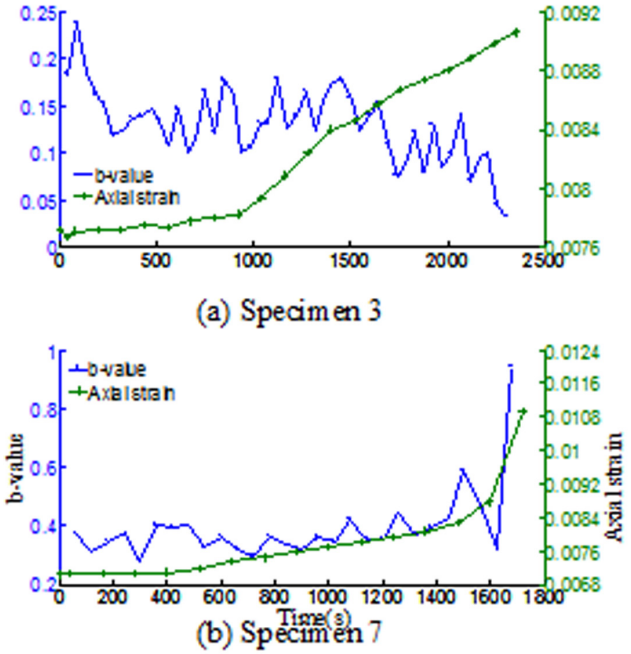

Fig 6. The b-value characteristics under the fifth constant load

By observing the changes of the specimen in the fifth grade of constant load, it can be found that cracks in Type I specimen surface are connected to each other and eventually form a macroscopic shear plane, ultimately leading to the shear instability of the test specimens. Cracks in Type II specimen surface are also connected to each other, thus squeezing out some filling materials around the waste rocks from the specimen even with, ultimately leading to the tensor instability of the test specimens. Again combined with the corresponding change features of acoustic emission b-value, it can be considered that when the acoustic emission b-values are constantly

making jagged upward fluctuations, the alternating small-scale and large-scale destruction suggests that the specimen is in the continuous connection among micro-cracks. The overall acoustic emission b-values tended to decrease, meaning that the continual connection process between micro-cracks is mainly large-scale micro-cracking, thus forming macroscopic shear surface. The overall acoustic emission b-values tended to increase, meaning that the continual connection process between micro-cracks is mainly small-scale micro-cracking, thus opening waste rocks in the specimen.

Conclusions

(1) According to the destruction mode, cemented waste rock backfills are divided into two types: shearing instability type (Type I) and tensor instability type (Type II). Short-term graded creep tests are respectively carried out on the two kinds of cemented waste rock backfill specimens. The results showed that both types of specimens are maintained in the volume deformation and volume constant states, and only Type-II specimens are in the expansion state.

(2) In the constant load that does not cause specimen instability, there is a close relationship between acoustic emission b-value and volume strain. When the specimen is in the decelerating creep phrase of the volume deformation stage, acoustic emission b-value shows a decreasing trend, indicating that the microcracks inside the specimen in the decelerating creep phase is mainly large-scale destruction. Also, in steady creep stage and the entire volume constant phase of the volume deformation stage, the overall acoustic emission b-value no longer significantly reduces, but fluctuates up and down. Besides, the variance is not large, indicating that microcracks in the specimen are in a steady expansion stage in these two stages. In the steady creep stage of the volume deformation stage, as the dead load increases, the variance of acoustic emission b-values of Type I specimen keep decreasing while that of Type II specimen is continuously increasing, indicating that as the dead load increases, the expansion of micro-cracks in Type I specimen is more stable while that of Type II specimen is getting intense.

(3) In the steady creep stage before specimen instability, the acoustic emission b-values of these two types of specimens are constantly making jagged upward fluctuations. The alternating small-scale and large-scale destruction suggests that the specimen is in the continuous connection among micro-cracks. In the steady creep and accelerating creep stages before specimen instablity, the acoustic emission b-values of Type I specimen shows a circulation pattern “jagged upward fluctuation - dramatic decrease”, signifying that the continual connection process between micro-cracks is mainly large-scale micro-cracking, thus forming macroscopic shear surface and causing the specimen to be instable. In the steady creep and accelerating creep stages before the specimen instability, the acoustic emission b-values of Type II are constantly increasing and making jagged upward fluctuations in the accelerating creep stage, meaning that the continual connection process between micro-cracks is mainly small-scale micro-cracking, thus opening waste rocks in the specimen.

Acknowledgment

This work is supported by the National Natural Science Fund, China (No. 51304083) and the national science and technology support program (No. 2013BAB02B08.

References

1. HE Gui-cheng, LIU Yong, DING De-xin, etal. Strength characteristic of cemeted waste rock backfills and its application. Journal of Mining & Safety Engineering, 2013, 30 p.p.74-79.
2. Guo L J, Yang X C. Test Study on Cemented Rock-tailings Filling. Journal of Wuhan Wniversity of Technology, 2008, 30, p.p.75-78.
3. Liu Z X, Li X B, Dai T G. On damage model of cemented tailings backfill and its match with rock mass. Rock and Soil Mechanics, 2006, 27, p.p.1442-1446.
4. Wang X J, Zeng J, Qin Y H, et al. Test and Study of Filling Body Quality Based on Sonic Wave Velocity Measurement. Science Technology and Engineering, 2007, 7, p.p.6180-6181.
5. Deng D Q, Gao Y T, Wu S C, Yu J W, et al. Experimental study of destructive energy dissipation properties of backfill under complicated stress condition. Rock and Soil Mechanics, 2010, 31, p.p.737-742.
6. LIN Feng, LI Shu-lin, XUE Yun-liang. Relationship between acoustic emission parameter and mechanics parameters damage degree of concrete material. Journal of Xiamen University(Natural Science), 2010, 49, p.p.526-530.
7. ZHU Hong-ping , XU Wen-sheng , CHEN Xiao-qiang ,et all. Quantitative concrete-damage evaluation by acoustic emission information and rate-process theory. Engineering Mechanics, 2008, 25, p.p.186-191.
8. WANG Xiaojun, FENG Xiao, ZHAO Kang (2011). Numerical simulation on acoustic

emission of roof fill failure of mining drift with different cross-section. MINING R&D, 2011, 31, p.p.9-11.
9. GONG Cong, LI Changhong, ZHAO Kui. Experimental study on b-value characteristics of acoustic emission of cemented filling body under loading and unloading test. Journal of Mining & Safety Engineering, 2014, 31, p.p.788-794.
10. Lochner D A, Byerlee J D, Kuksenko V, et al. Quasi-static fault growth and shear fracture energy in granite. Nature, 1991, 350, p.p.39-42.
11. LI Hong-yan, KANG Li-jun, XU Zi-jie, et al. Precursor information analysis on acoustic emission of coal with different outberst proneness. JOURNAL OF CHINA COAL SOCIETY, 2014, 39, p.p.384-388.
12. LI Yuan-hui, LIU Jian-po, ZHAO Xing-dong, et al. Study on b-value and fractal dimension od acoustic emission during rock failure process. Rock and Soil Mechanics, 2009, 30, p.p.2559-2574.
13. TANG Shao-hui, PAN Yi, WEN Xing. Experimental study on the rock damage and rupture process and coupling Law of AE features. Journal of Hunan University of Science & Technology(Natural Science Edition), 2012, 27, p.p.35-40.
14. Zeng Zhengwen, Ma Jin, Liu Liqiang, et al. AE b-VALUE DYNAMIC FEATURES DURING ROCKMASS FRACTURING AND THEIR SIGNIFICANCES. SEISMOLOGY AND GEOLOGY, 1995, 17, p.p.7-12.

The advance research of organic silane rubber asphalt stabilizer

Bai Niuniu[1], Ling Binshang[1], XiaoRenping[1], LiJing[1,2], LiXin[1], ZhangXiangmin[1]

[1]Guangxi Colleges and Universities Key Laboratory of New Technology and Application in Resource Chemical Engineering, School of Chemistry and Chemical Engineering, Guangxi University, Nanning 530004, China
[2]Guangxi Key Laboratory of Petrochemical Resource Processing and Process Intensification Technology, Guangxi University, Nanning 530004, China Email:836636913@qq.com

Corresponding author is LiJing

Abstract
The causes of rubber asphalt and rubber asphalt stabilizer are analyzed, and the compatibility between rubber asphalt is to determine the service life of rubber asphalt. and a detailed introduction of the research progress of several kinds of rubber asphalt stabilizer, finally the development of rubber asphalt stabilizer of future prospects. Organic silane coupling agent has many unique physical properties and chemical properties, these properties,